

A MODEL FOR STELLAR SURFACE CONVECTION AND PHOTOSPHERIC LINE ASYMMETRIES

H. M. ANTIA

Tata Institute of Fundamental Research

AND

S. K. PANDEY

Ravishankar University

Received 1988 July 18; accepted 1988 October 27

ABSTRACT

A model for stellar convection zones based on linear convective modes using a nonlocal mixing length theory is developed to study the spectral line asymmetries resulting from convective motions in the stellar photospheric region. The amplitudes of these linear convective modes is estimated by demanding that the convective flux due to a linear superposition of such modes should reproduce the convective flux required by the mixing length model. The mode with the largest amplitude in the photospheric line formation region is chosen to represent the stellar surface structure. Synthetic spectral line profiles are obtained by summing locally symmetric profiles over the stellar disk according to the local Doppler velocity and intensity fluctuations. Four stars, i.e., the Sun, α Cen A, Arcturus, and Procyon, which have characteristically different observed line bisector shapes are chosen for the study. It is found that the simple model considered here can explain the gross features of the observed bisector shapes for these stars of different spectral types.

Subject headings: convection — line profiles — stars: atmospheres — Sun: atmospheric motions

I. INTRODUCTION

Convection in the solar envelope manifests itself in the form of granulation and supergranulation. It will be difficult to observe such features on the surface of other stars. However, long before granulation was identified as convective cell it was found that the solar lines are actually shifted with respect to the laboratory wavelengths. This was later on shown to be due to convection since the brighter granules which have upward velocity contribute more flux than the darker intergranular lanes. Apart from blueshift, this also introduces a small but measurable asymmetry in the spectral lines. This asymmetry can be most conveniently characterized in terms of the line bisector which is the loci of points midway between equal intensity points on either side of the line.

For solar lines the convective blueshift is $\sim 0.5 \text{ km s}^{-1}$, while the bisector shape is convex toward the blue side somewhat like the letter "C." A detailed study of the solar line bisectors has been carried out by various workers (see Dravins 1982, and references therein). Such studies can, in principle, be carried out for other stars since the asymmetry is present even in the solar lines integrated over the entire solar disk (Bray and Loughhead 1978). However, since a very high resolution spectrum is required to study the small asymmetries in the spectral lines, only the bright stars can be considered for such a study. Asymmetries in the spectral lines of Arcturus and Procyon were detected by Gray (1980, 1981). Recently, Dravins (1987) has studied the line bisectors for some of the bright stars. These studies show that the stars of different spectral types are characterized by quite different line bisector shapes.

Theoretical models incorporating convective velocities have been constructed to obtain synthetic line profiles which can be compared with the observed profiles. Such studies will enable us to learn more about the process of stellar convection. Most of these models have been based on simple two to four-stream models (Schrüter 1957; Beckers and Nelson 1978; Dravins

1988) where the stellar surface is divided into two to four components of different characteristic brightness and velocity. The synthetic line profile is obtained as a summation of line profiles from these components appropriately weighted for their area coverage. Velocities and brightness, as well as the relative areas of different zones, are adjusted to produce synthetic line bisectors which are close to observed ones. Using a two-component model, Gray and Toner (1985) inferred that, for main-sequence F and G stars, granulation velocities increase with the increasing effective temperature. On the other hand, Dravins, Lindgren, and Nordlund (1981) and Dravins and Nordlund (1986) have constructed a more sophisticated model of convection zone by actually solving the set of hydrodynamic equations for solar granulation. Because of constraints imposed by computer time, such models have to be restricted in extent; further, the small-scale turbulence cannot be accounted for. However, such models give detailed convective velocity field and hence can be used to construct synthetic line profiles using the equation of radiative transfer. These models have essentially no free parameter and can provide a good test for the hypothesis of convective origin of spectral line asymmetries.

In this paper we propose a model of stellar convection zone in terms of linear convective modes. This model has the advantage of being simpler than the full simulation models of Nordlund (1982), and it can provide a velocity field over the entire stellar volume. The linear convective modes in the solar convection zone have been studied by Antia, Chitre, and Narasimha (1983), and it was found that there are two peaks in the growth rate versus horizontal wavelength plot which are in a reasonable agreement with the observed length and time scales of granulation and supergranulation. The linear stability theory used in this approach does not give the amplitudes of these modes which can only be determined by nonlinear processes. However, it is reasonable to assume that the convective flux will be transported by a combination of these modes.

Narasimha and Antia (1982, hereinafter NA) have demonstrated that it is possible to construct a linear superposition of statistically independent unstable convective modes which reproduces convective flux as required by the mixing length theory over the entire convection zone. The resultant vertical velocities were found to be in a reasonable agreement with the observed granular velocities in the solar atmosphere. This may not provide a fully realistic model of stellar convection zone since it is based on the mixing length theory which itself is uncertain to a large extent. However, it can provide a reasonable first approximation to stellar convection zone.

In this study we have attempted to construct convection zone models for four of the stars studied by Dravins (1987): the Sun, α Cen A, Arcturus, and Procyon. These stars show significantly different line bisector shapes; hence, it would be interesting to identify the differences in the structure of convection zone which are responsible for the variation in line profiles. Apart from this, we also attempt to identify the characteristic sizes, lifetimes, and velocities for convective cells in these stars.

The rest of the paper is organized as follows: in § II we describe the convection zone model; in § III we discuss the construction of synthetic line profiles; in § IV we present the numerical results for convection zone models for the four stars and, using these models, the synthetic line profiles are constructed. Finally, § V summarizes the conclusions of the present work.

II. CONVECTION ZONE MODELS

The equilibrium models for the stellar envelopes of the four stars, viz. the Sun, α Cen A, Arcturus, and Procyon, are constructed by using a nonlocal mixing length theory of convection including turbulent pressure as described by Antia, Chitre, and Narasimha (1984, hereinafter ACN). We have used the solar composition ($X = 0.732$, $Y = 0.25$, $Z = 0.018$) for α Cen A and Procyon, while for Arcturus we have taken $X = 0.732$, $Y = 0.258$, $Z = 0.01$. The basic stellar parameters as given in Allen (1973) are used, except for the mass of Arcturus which is taken from Bell, Edvardsson, and Gustafsson (1985).

The linear stability of these models is investigated using the equations as described in ACN. This gives a series of convective modes for different values of the degree of spherical harmonics l . The width of the flux profile for these modes can be compared with the mixing length as shown in ACN. The value of mixing length used in the mixing length theory can be adjusted so as to agree with the width of the dominant convective mode at the corresponding depth. For the width of the convective flux profile we have used the equivalent width as defined in Equation (18) of ACN, but to avoid confusion with the equivalent width of the spectral lines we shall refer to it simply as width. Instead of this, we could have used the full width at half-maximum of the flux profile or any other suitable measure of its width.

The linear stability analysis does not give the amplitude of these modes in the stellar envelope. To determine the amplitudes of these modes we use a procedure described in NA, where it was shown that it is possible to find a linear superposition of statistically independent unstable convective modes which reproduces the convective flux as required by the mixing length theory in the entire convection zone. For constructing such a linear superposition we choose a sample of ~ 15 representative modes spanning the entire range of l -values for which unstable convective modes exist. The amplitudes of these modes are then determined by doing a least-squares fit to the

convective flux profile predicted by the mixing length theory. This procedure has some limitations since the problem of finding a minimum of a function of 15 variables is nontrivial and usually does not lead to results which vary smoothly with l . However, gross properties of convection zone may be modeled reasonably well. This approach fixes the amplitude of the convective modes, but it cannot specify the relative phases between the various modes. As a result, the sign of various terms in the linear superposition remains arbitrary. To avoid this arbitrariness we use only the dominant convective mode to construct the synthetic line profiles. For this purpose we choose the mode which has largest velocity and flux perturbations in the line formation region which lies above the photosphere.

Apart from convection, there are other velocity fields in the stellar atmosphere like those due to oscillations and small-scale turbulence. Most of these contribute to the line broadening but little to asymmetry because either they have insufficient intensity contrast, or the intensity fluctuations are not sufficiently in phase with the velocity. Hence we do not include such velocity fields in construction of synthetic line profiles.

III. SYNTHETIC LINE PROFILES

Using the velocity field provided by the convection zone model, we construct synthetic line profiles by integrating over the entire stellar surface. At each point on the stellar surface the line profile is assumed to be symmetric, the actual form being given by the usual Voigt function. The elementary Voigt profiles were computed from the series expansion (Allen 1973):

$$V(\Delta\lambda) = H_0(\Delta\lambda) + aH_1(\Delta\lambda) + a^2H_2(\Delta\lambda) + a^3H_3(\Delta\lambda) + a^4H_4(\Delta\lambda), \quad (1)$$

where $V(\Delta\lambda)$ is the intensity at wavelength shift of $\Delta\lambda$ with respect to the line center in some arbitrary units, a is a parameter giving the ratio of Lorentzian to Gaussian width. The functions H_0 , H_2 , H_3 , and H_4 are taken from Mihalas (1978). We have used a typical value of 0.01 for the parameter a which should be applicable to a fairly strong line. Further, at the extreme wings of the line profile we have used a purely Lorentzian profile which merges with the Voigt profile at $\Delta\lambda = \pm 6$ km s⁻¹. A typical value of 5000 Å is used for the wavelength while constructing synthetic line profiles.

To construct the synthetic line profile we integrate the intensity over the entire surface taking into account the Doppler shift due to convective velocity. For simplicity we assume that the perturbation is axisymmetric about the line of sight, and the integrated intensity is given by

$$I(\lambda) = \int_0^{\pi/2} \cos \theta I(\theta, \lambda) 2\pi \sin \theta d\theta. \quad (2)$$

The intensity $I(\theta, \lambda)$ at the position characterized by angle θ and wavelength λ can be written as (Fig. 1)

$$I(\theta, \lambda) = V \left\{ \lambda - \lambda_0 + \frac{\lambda_0}{c} [v_r(\theta) \cos \theta - v_h(\theta) \sin \theta] \right\} \times \left(1 + \frac{\Delta F(\theta)}{F} \right) S(\theta), \quad (3)$$

where λ_0 is the wavelength of the line, c is the velocity of light, v_r and v_h are, respectively, the radial and horizontal components of velocity, ΔF is the flux fluctuation due to the con-

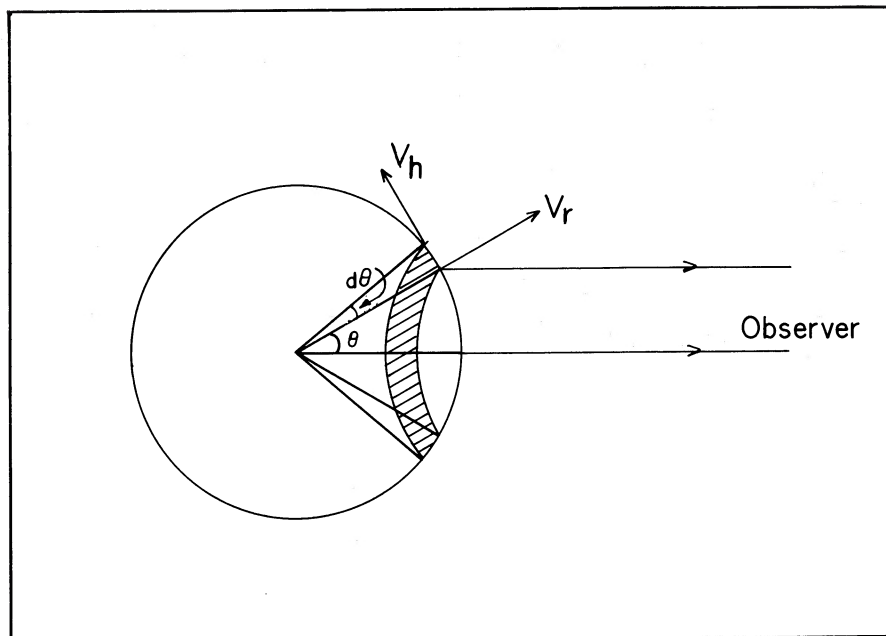


FIG. 1.—Diagram illustrating the geometry used to compute the integrated line profiles

vective mode, F is the average stellar flux, $S(\theta)$ is the limb darkening function given by

$$S(\theta) = 1 - u_2 - v_2 + u_2 \cos \theta + v_2 \cos^2 \theta, \quad (4)$$

where the values of u_2 and v_2 are taken from Allen (1973). Since we are considering only one convective mode, we can write

$$\begin{aligned} v_r &= \sqrt{l + \frac{1}{2}} V_r P_l(\cos \theta), \\ \Delta F &= \sqrt{l + \frac{1}{2}} F_1 P_l(\cos \theta), \\ v_h &= \sqrt{\frac{2l + 1}{2l(l + 1)}} V_h \frac{d}{d\theta} [P_l(\cos \theta)], \end{aligned} \quad (5)$$

where V_r and V_h are the amplitudes of vertical and horizontal components of velocity and F_1 is the amplitude of flux perturbation of the convective mode with degree l .

IV. NUMERICAL RESULTS

The linear stability of equilibrium stellar envelope model is studied by solving the equations as given in ACN for convective modes with different values of the degree l . These linearized equations involve the turbulent Prandtl number (σ_t) which is essentially a free parameter of order unity. However, the requirement of consistency of mixing length theory does put

some constraints on the value of this parameter as explained later in this section. The value of Prandtl number actually used in the results presented here is given in Table 1 along with other parameters of the equilibrium model. For each value of l there could be more than one unstable convective modes. These modes are identified by C1, C2, ..., in order of decreasing growth rates. For the Sun and α Cen A only the C1 mode is unstable, while for Arcturus and Procyon C2 and for some values of l even the C3 mode can be unstable.

Figure 2 shows the growth rate of these modes as a function of l , for all the four stars. It can be seen that the Sun, α Cen A, and Arcturus display double peak curves, while Procyon shows only one peak for each series of modes. For Arcturus the second peak occurs at $l = 1$ and may not be easily visible in the figure. This feature is consistent with the general reduction in value of l or corresponding increase in the length scales for giant stars (ACN). It is reasonable to expect that the mode with maximum growth rate will dominate in the convection zone. This could give the dominant length and time scales of convection in these stars. Table 1 summarizes the results of these calculations. For the Sun the length and time scales corresponding to the two peaks roughly agree with the observed values for granulation and supergranulation. This could be compared with the results of Antia, Chitre, and Narasimha

TABLE 1
PROPERTIES OF STELLAR ENVELOPE MODELS

Star	Luminosity (L_\odot)	Mass (M_\odot)	Effective Temperature (K)	Mixing Length	Depth of Convection Zone (km)	Prandtl Number	λ_1 (km)	T_1 (hr)	λ_2 (km)	T_2 (hr)
Sun	1	1	5770	$z + 459$ km	1.84×10^5	0.33	3.8×10^3	0.70	4.0×10^4	62
α Cen A	1.56	1.1	5811	$z + 613$ km	2.07×10^5	0.50	5.9×10^3	0.95	9.0×10^4	159
Arcturus	102.8	0.95	4375	$2.5H_p$	1.17×10^7	0.75	1.5×10^7	76	5.0×10^7	5500
Procyon	7.52	1.77	7328	$1H_p$	1.28×10^3	0.50	1.2×10^4	1	4.1×10^3	8

NOTE.—Here λ_1, λ_2 are horizontal wavelengths of modes corresponding to peaks in the l vs. growth rate plots, and T_1, T_2 are the corresponding time scales: z is the depth measured from level with optical depth $\frac{2}{3}$.

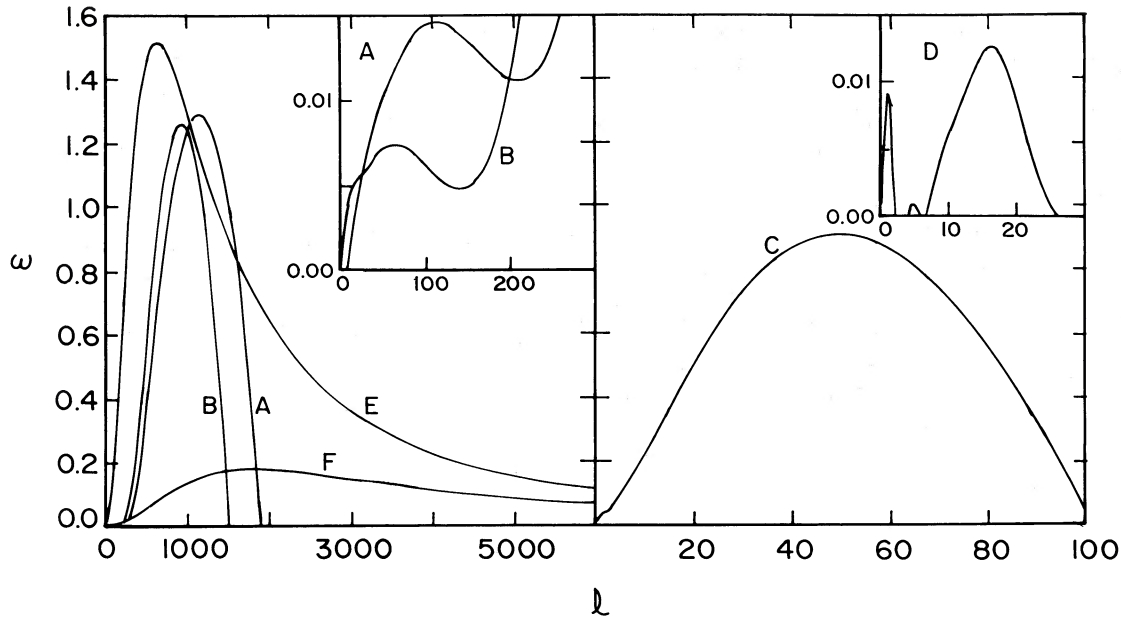


FIG. 2.—The growth rate ω [in units of $(3GM/4\pi R^3)^{1/2}$] of convective modes as a function of the degree of spherical harmonics l for all the four stars; the Sun (C1 mode, A), α Cen A (C1 mode, B), Arcturus (C1 mode, C; C2 mode, D), and Procyon (C1 mode, E; C2 mode, F).

(1983) where the length and time scales corresponding to the primary maximum in the growth rate were found to be somewhat smaller. This variation could be due to the usage of a slightly different version of mixing length formulation in this work. It may be noted that here we have used somewhat larger value for the parameter $c (= 1)$ which is the ratio of turbulent pressure to ρW^2 , where ρ is the density and W the convective velocity. Reducing this parameter will decrease the length and time scales of the dominant modes. If the value of turbulent Prandtl number is reduced, then the growth rate versus l plot may have only one peak. This in some sense puts a lower limit on the value of σ_t , since we would like to have two distinct scales for solar convection. This, along with the upper limit on σ_t , provided by the consistency requirement discussed later on, essentially fixes this parameter. For α Cen A the results are not very different, the length and time scales for granulation and supergranulation on α Cen A comes out to be somewhat larger than that for the Sun.

For Arcturus the maximum growth rate occurs at a much lower value of l as compared to that for the Sun or α Cen A, thus giving a much larger length scale for convection. Arcturus is a cool giant with very low density in the envelope, and consequently the superadiabatic gradient throughout the convection zone is significantly high. Further, because of low surface gravity the scale height is very large in the envelope which produces correspondingly larger horizontal scales for the dominant convective mode. It may be noted that the pressure scale height in the solar convection zone varies from 150 km at the top to $\sim 60,000$ km at the bottom, a variation by a factor of 400. This contrasts with Arcturus where the scale height variation is about a factor of 10, ranging from 100,000 km at the top to a maximum of $\sim 1,000,000$ km in the convection zone. On the other hand, Procyon being a hotter star, the convection zone is very shallow, and in fact it has two shallow convection zones. The second convection zone, which is

between the depth of 6800 to 9700 km, is not included in Table 1. Since we are interested in the amplitudes of convective modes near the photosphere we have considered the convective modes in the upper convection zone only. These modes may penetrate into the lower convection zone changing their characteristics to some extent, but we have ignored this effect for simplicity.

To obtain the amplitudes of these linear convective modes we attempt a least-squares fit to mixing length flux profile as explained in § II. The results for α Cen A, Arcturus, and Procyon are shown in Figure 3, while the results for the Sun have already been published in NA. This figure also shows the convective flux profiles of some of the individual convective modes. It can be seen that the modes with different values of l have peaks at different depths. This enables us to construct a linear superposition of convective modes which reproduces the convective flux as required by the mixing length formulation over the entire convection zone. The consistency requirement also puts some constraints on the value of σ_t , since a good fit to the model flux cannot be obtained for all values of σ_t . For the Sun and α Cen A, if σ_t is increased beyond the values used in these calculations, then the growth rate for some range of values of l between the two peaks (Fig. 2) can become negative. This in turn will wipe out the corresponding range of l -values from the set of unstable convective modes used for fitting the model convective flux. This implies that for certain range of depth in the convection zone there are no convective modes having maxima there, and as a result it will not be possible to get a good fit to the model convective flux. It is thus possible to fix an upper limit on σ_t . For Arcturus we have also tried the calculations with lower values of σ_t , and found that there was a large gap between the maxima for $l = 1$ and $l = 2$ modes, thus giving a significant dip in the superposed convective flux profile. By increasing the Prandtl number to a value given in the Table 1, the peak due to the C2 mode shifted to some

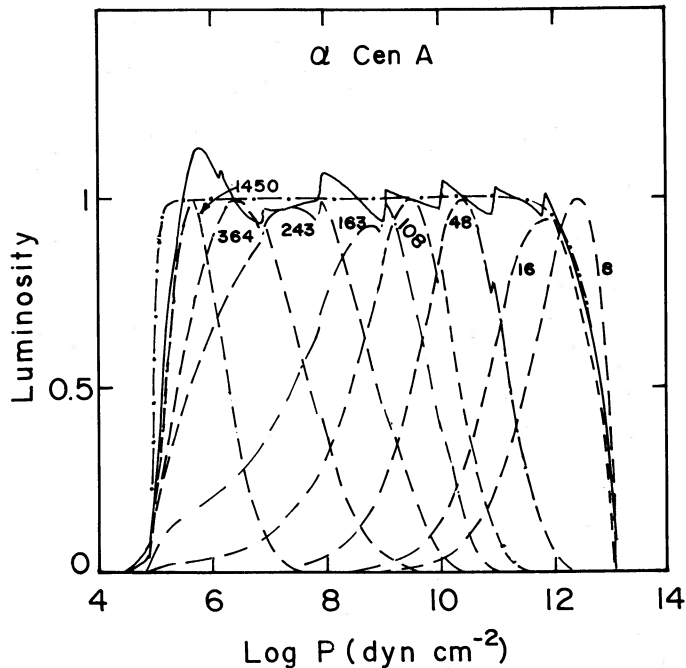


FIG. 3a

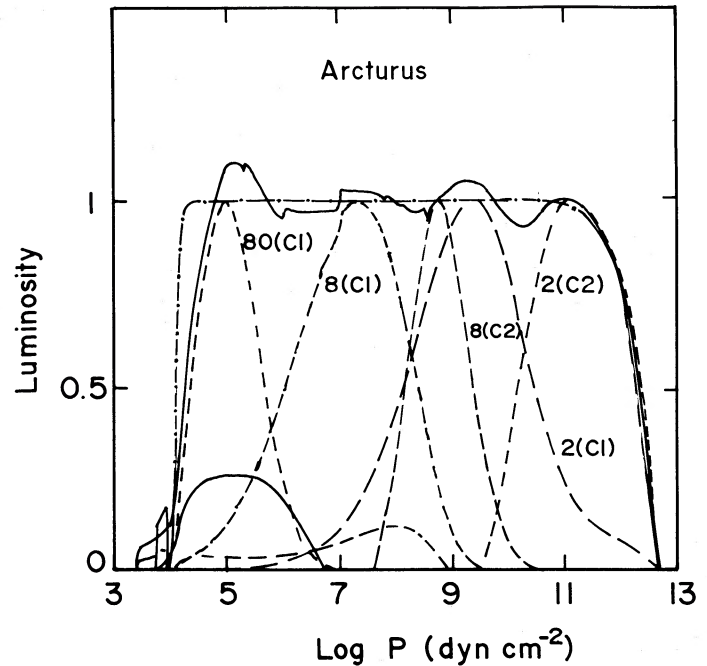


FIG. 3b

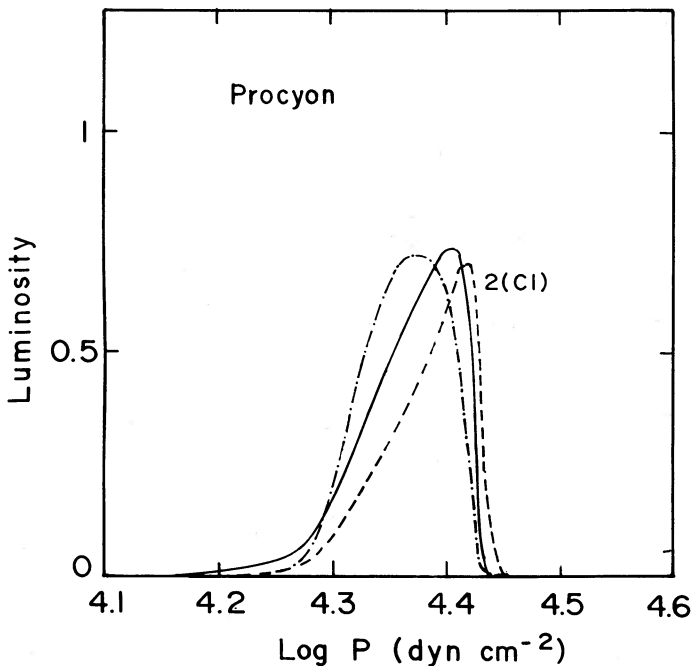


FIG. 3c

FIG. 3.—(a) Dashed curves show the convective luminosity due to individual convective modes for various l -values as a function of logarithm of pressure for α Cen A. The continuous curve shows superposed convective luminosity profile, while the dot-dashed curve represents the model convective luminosity. The luminosity is expressed in terms of stellar luminosity. (b) Dashed curves show the convective luminosity due to individual convective modes for various l -values as a function of logarithm of pressure for Arcturus. The continuous curve shows superposed convective luminosity profile, while the dot-dashed curve represents the model convective luminosity. The luminosity is expressed in terms of stellar luminosity. (c) The dashed curve shows the convective luminosity due to C1 mode for $l=2$ as a function of logarithm of pressure for Procyon. The curves for higher l values more or less coincide with the continuous curve showing superposed convective luminosity and hence are not displayed in this figure. The dot-dashed curve represents the model convective luminosity. The luminosity is expressed in terms of stellar luminosity.

extent, thus enabling us to get a better fit. For Procyon all the convective modes have peaks at nearly the same depth, which essentially coincide with the peak in the model convective flux. Hence it is not possible to construct a unique superposition of convective modes which matches the model convective flux. As a result, the amplitudes of these modes cannot be fixed uniquely.

Following ACN, we attempt to identify the mixing length with the width of the flux profile for the dominant convective mode at the corresponding depth. Here the dominant mode is

the one which has the maxima of flux profile at that depth. The results for the Sun, α Cen A, and Arcturus are shown in Figure 4, while for Procyon it is not possible to use this approach since all the modes have maxima at the same depth. It can be seen that there is a general agreement between the mixing length and the width of the dominant convective mode. We would like to point out that we had constructed models for Arcturus using mixing length of $1H_p$ and $2H_p$, also, but the width was found to be much larger than the mixing length. Therefore we have used a higher value for the mixing length. A

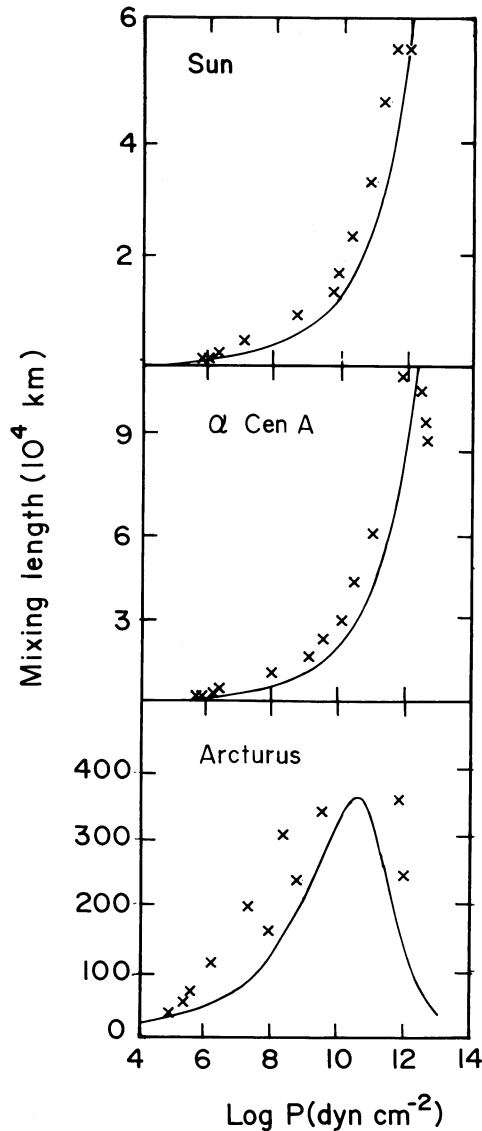


FIG. 4.—The mixing length is plotted against logarithm of pressure for the Sun, α Cen A, and Arcturus. The width of the luminosity profile of various convective modes is indicated by crosses.

better agreement between the mixing length and the width can possibly be obtained if we allow the ratio of mixing length and pressure scale height to vary with depth.

The amplitudes of velocity and flux fluctuations due to various convective modes at a optical depth of 0.4 are given in Table 2. As noted earlier, the amplitudes cannot be determined for Procyon; hence, in that case we have listed the amplitudes which will result if the convective flux profile due to an individual mode is normalized to give the same maximum as the model flux profile. Consequently the actual amplitudes of these modes will be smaller than the tabulated values. Further, for Procyon it was found that the eigenfunction for the radial velocity has a node very close to the optical depth of 0.4 for

quite a few of the modes, and hence the value of V_r may be underestimated. Also depending on the depth of line formation the relative phase of vertical velocity with respect to other variables could be different.

It should be noted that only those modes which were used for fitting the model flux profile are included in the table. Each of these modes is supposed to include the contributions from the neighboring modes; hence, the exact value of l should not be taken too seriously. The amplitudes will also depend on which values of l are included for fitting; hence, the tabulated results can only be a rough estimate of the actual amplitudes. Further, the signs of the amplitudes in the table specify the relative phases of various quantities as determined by the corresponding eigenfunctions. The flux perturbations in this table refer to the stellar flux averaged over the entire spectrum, while in constructing line profiles we would be interested in the fluctuations in the line intensity at the given wavelength. This could be completely different from the values in Table 2, since it will depend on the relative change between the continuum and line flux. Hence, the amplitude of flux perturbation can be regarded as a free parameter in our model. We have used some plausible values for this parameter.

From the Table 2 it can be seen that for the Sun, velocity and flux perturbations are dominated by the mode with $l = 1540$. Apart from this, the mode with $l = 364$ also has a comparable contribution. For α Cen A the major contributions to velocity and flux fluctuation come from modes with $l = 243$ and 1230, as seen from Table 2. This is very similar to the solar case. It is interesting to note that the horizontal velocity component due to C2 modes was found to be abnormally large (Narasimha and Antia 1982) when the turbulent pressure was not incorporated in the stability analysis. The inclusion of turbulent pressure in the present study wipes out the C2 modes as their growth rates become negative, thus removing the unrealistically large contribution to horizontal velocity. It may be noted that the two dominant values of l are somewhat larger than those corresponding to the two peaks in Figure 2, for both these stars. This may justify our identification of the two peaks with the two dominant scales of solar convection. The length scales appear to be slightly smaller than those presented in Table 1, which will improve the agreement with observed length scales of granulation and supergranulation. From Table 2 it can be seen that for the Sun the amplitudes of the flux perturbations are smaller for $l \approx 350$ as compared to that for $l \approx 1500$. This is in qualitative agreement with observations, which show that the intensity contrast for granulation is much larger than that for supergranulation. For the cool giant Arcturus the modes for low l -values in the range of 4–8 dominate the fluctuations, as is evident from Table 2. Apart from this, the C1 mode for $l = 50$ makes significant contribution to the perturbations. Once again these two length scales are somewhat larger than those quoted in Table 1. For the hotter main-sequence star Procyon, the amplitudes cannot be determined by the fitting procedure. However, the convection zone for Procyon is very shallow; hence, we would expect modes with small horizontal scales to dominate. Further, our results for the other stars suggest that maximum amplitudes are obtained for modes with somewhat smaller length scales as compared to those obtained from the peaks in Figure 2. Both these considerations suggest that modes with large values of $l \approx 2000$ will dominate. It can be seen from Table 2 that for $l \approx 2000$ the vertical component of velocity is in phase with the horizontal velocity. For some of the higher values of $l (\geq 1000) V_r$ is out of

TABLE 2
 AMPLITUDES OF VELOCITY AND FLUX PERTURBATIONS FOR CONVECTIVE MODES AT OPTICAL DEPTH = 0.4

SUN												α Cen A												ARCTURUS												PROCYON											
SUN				α Cen A				ARCTURUS				PROCYON				SUN				α Cen A				ARCTURUS				PROCYON																			
<i>l</i>	<i>V_r</i>	<i>V_h</i>	<i>F₁/F</i>																																												
10	3	-809	6	8	1	-208	1	2	0.02	-1	0.03	2	1110	-2280	440	2	1370	-3600000	4800	20	-88	-918000	6220																								
20	1	-115	2	16	5	-649	9	4	0.40	-15	1	4	2790	-2700	1090	20	1350	-419000	4610	200	-360	-108000	6240																								
30	3	-322	6	32	8	-403	15	8	259	-5110	453	8	1820	-2400	802	200	1190	-35900	3140	1000	-753	-26800	6500																								
45	5	-348	10	48	33	-842	54	16	9	-92	14	16	907	-1320	449	1000	864	-14300	6370	2000	-580	-14300	6530																								
72	23	-1100	51	72	75	-996	110	32	1	-1	1	2000	-134	-12700	6550	6000	1220	-4560	5300																								
108	23	-757	52	108	168	-1160	240	50	1400	-4120	1140	6000	1230	-4550	5300																								
162	21	-539	53	162	433	-1970	610	80	1050	-1560	559																								
243	162	-3700	480	243	1190	-5830	1900																								
364	287	-5100	920	364	243	-1410	460																								
546	9	-102	27	546	36	-191	74																								
820	18	-148	51	820	5	-22	11																								
1000	6	-40	16	1230	1202	-3770	2400																								
1230	55	-360	150	1450	249	-720	490																								
1540	604	-3735	1650																								
1845	326	-2960	1200																								

NOTE.—Velocity amplitudes are in ms^{-1} , and F_1/F values are multiplied by 10^4 .

phase with V_h at optical depth = 0.4, but there is a node in vertical velocity eigenfunction just above this level. Hence, once again, over most of the line formation region the phase relation is same as that for $l = 2000$ mode. This phase relation is opposite to that in the other three stars and, hence, will affect the bisector shape.

Using the velocity and flux fluctuations due to dominant convective mode, the synthetic line profiles and bisectors are constructed using the formulation given in § III. However, since in general the asymmetry is very small, the bisector will not show any departure from a straight line on a normal plot. Hence, to display the shape of bisector, following Dravins (1987), we also plot the bisector on a scale which is 10 times the scale used for line profile. Further, the line profile and bisector are shifted so that the peak of the line profile occurs at zero wavelength in the plots. Hence, the shift of line profiles is suppressed in our plots. Figure 5 displays the resulting line profile and bisectors, while Figures 6a–6d show the bisectors on an expanded scale where, for clarity, the curves have been shifted horizontally so that they do not overlap each other.

Figure 6a shows the line bisectors resulting from $l = 100$ and 1500 modes, with different combinations of V_r , V_h , and F_1/F which are typical values for the Sun. From the second and the fourth bisectors in Figure 6a, which differ only in l -values, it is

clear that for this range of l -values the bisector shapes are independent of l . This can be expected from the properties of spherical harmonics which enter into the perturbed quantities (eq. [5]). Hence, we have used $l = 100$ for the Sun, α Cen A, and Procyon, to save computer time in evaluating the integrals. The line bisectors for the Sun, α Cen A, Arcturus, and Procyon are displayed in Figures 6a, 6b, 6c, and 6d, respectively. In each case we have used a few sets of values of the amplitudes of fluctuations which are close to the computed ones given in Table 2. The resulting shapes of line bisectors are similar to the observed profiles (Dravins 1987). The difference between the bisector shapes for the Sun and α Cen A are due to the somewhat larger amplitudes of the velocity. For Procyon the bisector shapes are significantly different as compared to the previous two stars because the vertical component of velocity is in phase with the horizontal component. The characteristically different shapes for Arcturus are due to the entirely different l -values for the dominant convective modes.

V. CONCLUSIONS

We have investigated the line profiles using a model of stellar convection zone based on linear convective modes. The resulting bisector shapes for the Sun, α Cen A, Arcturus, and Procyon can be compared with the observed shapes for these

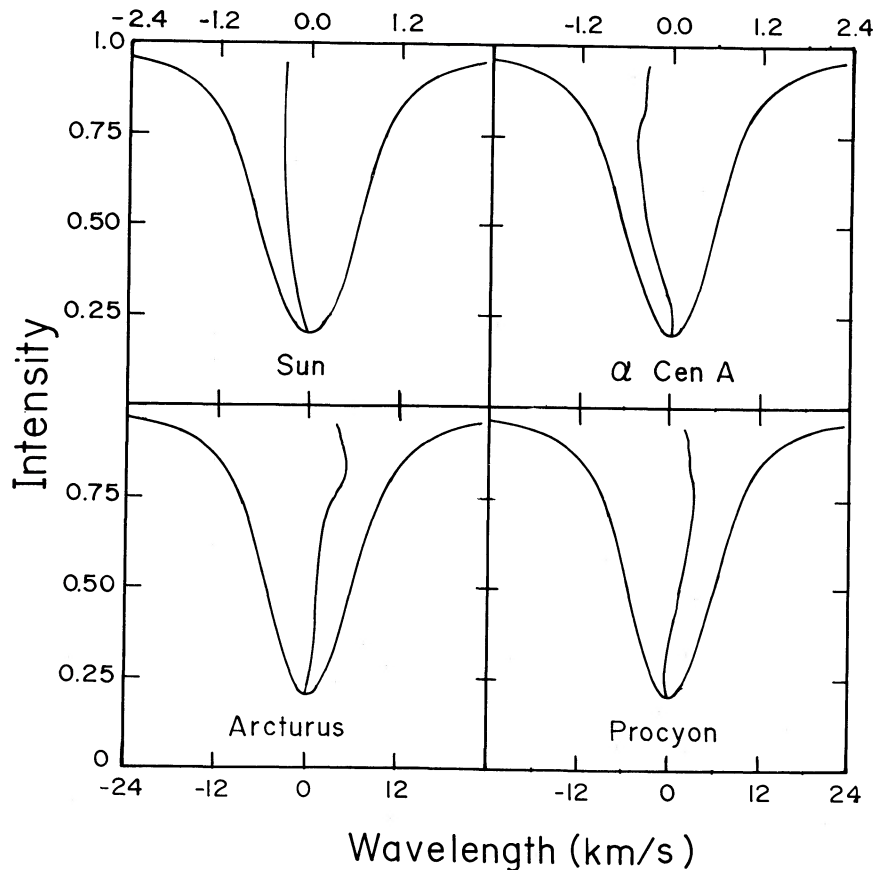


FIG. 5.—Representative synthetic line profiles and bisectors for various stars. The horizontal wavelength scale (in velocity units) refers to the line profile, while the 10 times expanded upper scale refers to the bisectors. The values of $(l, V_r, V_h, F_1/F)$ for various stars are: Sun (100, 1.5, -8, -0.2), α Cen A (100, 3, -6, -0.4), Arcturus (6, -4, 4, 0.2), Procyon (100, -2, -6, -0.5).

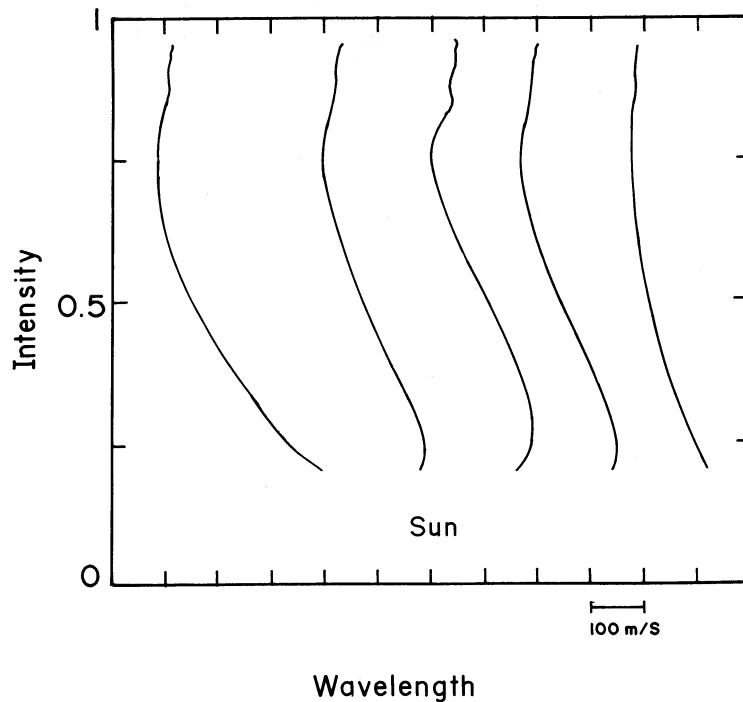


FIG. 6a

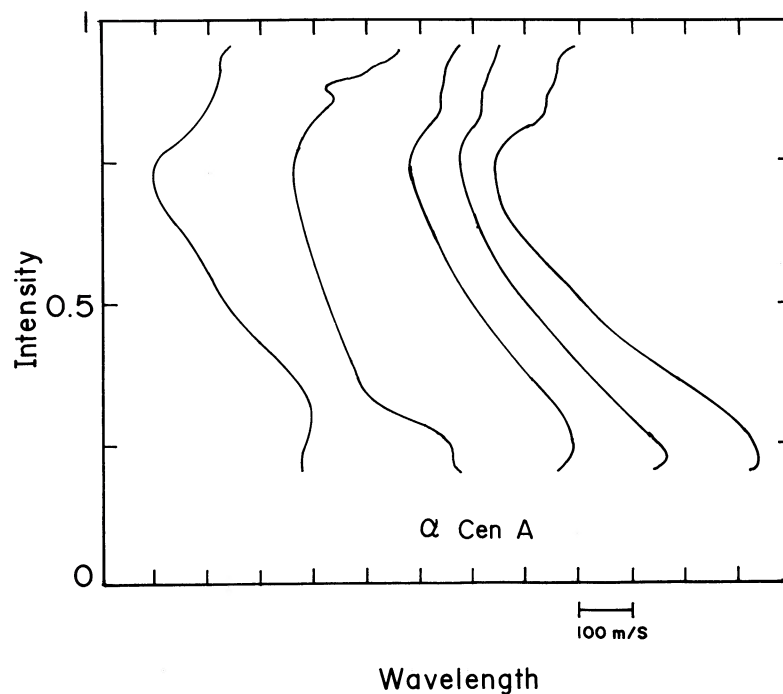


FIG. 6b

FIG. 6.—(a) Synthetic line bisectors for some typical values of the amplitudes of convective modes for the Sun. Curves have been shifted horizontally to avoid overlapping of the curves. The values of $(l, V_p, V_h, F_1/F)$ for various curves from left to right, are $(100, 1.5, -8, -0.2)$, $(1500, 1, -7, -0.3)$, $(100, 1.5, -6, -0.3)$, $(100, 1, -7, -0.3)$, $(100, 0.7, -8, -0.2)$. (b) Synthetic line bisectors for some typical values of the amplitudes of convective modes for α Cen A. Curves have been shifted horizontally to avoid overlapping of the curves. The values of $(l, V_p, V_h, F_1/F)$ for various curves from left to right, are $(100, 3, -5, -0.4)$, $(100, 5, -5, -0.2)$, $(100, 2.5, -6, -0.3)$, $(100, 2, -7, -0.3)$, $(100, 3, -6, -0.4)$. (c) Synthetic line bisectors for some typical values of the amplitudes of convective modes for Arcturus. Curves have been shifted horizontally to avoid overlapping of the curves. The values of $(l, V_p, V_h, F_1/F)$ for various curves from left to right are $(6, -3, 3, 0.2)$, $(3, -2, 4, 0.1)$, $(6, -4, 4, 0.2)$, $(3, -3, 3, 0.2)$, $(3, -3, 5, 0.2)$. (d) Synthetic line bisectors for some typical values of the amplitudes of convective modes for Procyon. Curves have been shifted horizontally to avoid overlapping of the curves. The values of $(l, V_p, V_h, F_1/F)$ for various curves from left to right, are $(100, -2, -5, -0.5)$, $(100, -2, -6, -0.5)$, $(100, -3, -6, -0.5)$, $(100, -1, -8, -0.4)$, $(100, -2, -7, -0.5)$.

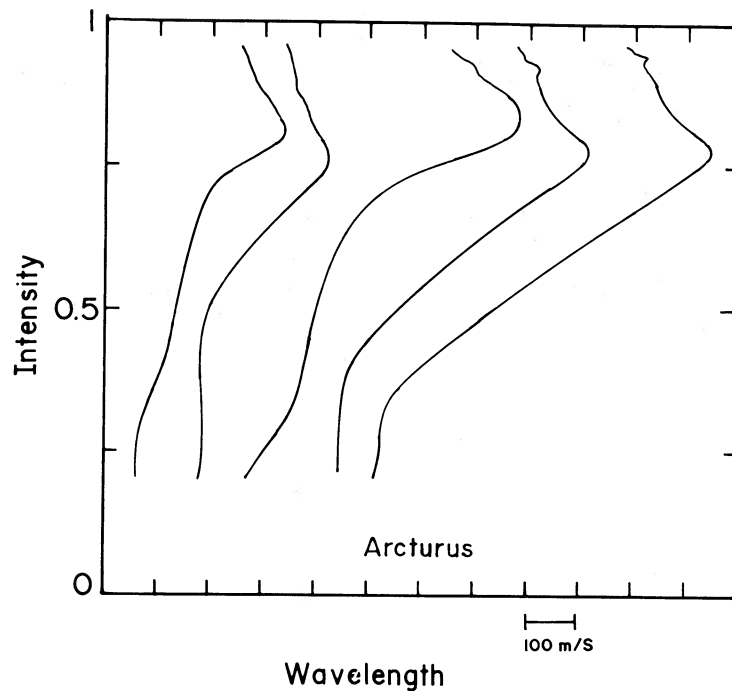


FIG. 6c

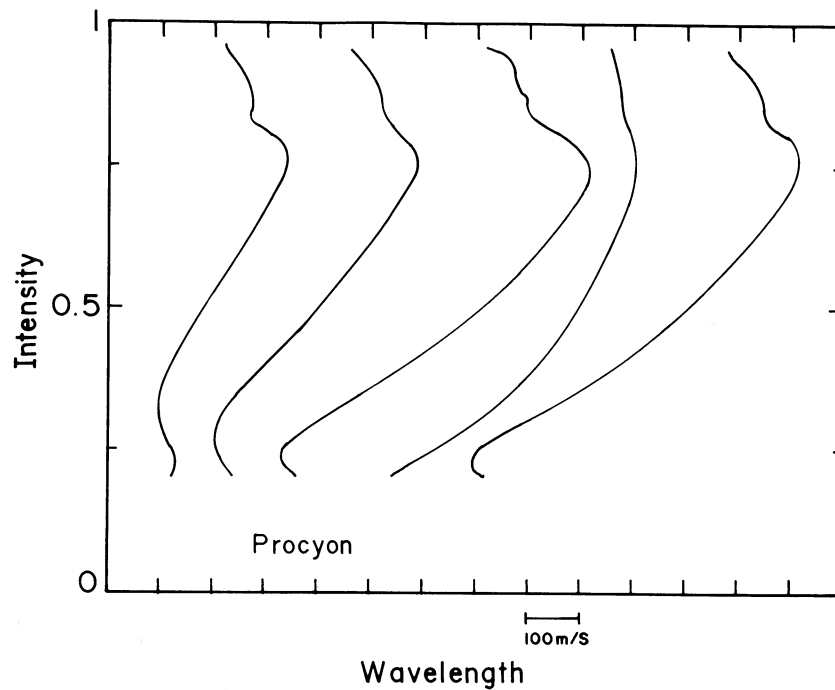


FIG. 6d

stars (Dravins 1987). The main characteristics of line bisectors are roughly reproduced by our synthetic line profiles. In our computations we have not taken into account the stellar rotation and the variation with height of velocity and flux fluctuations. The line width, as well as the line profile itself, will be a function of position on the stellar disk because of the temperature fluctuations. These factors may also affect the asymmetry of spectral lines. Besides, we have included the velocity and flux perturbations due to the dominant mode only, while

in reality the other modes will also contribute to these fluctuations. Hence, we cannot expect our line profiles to match exactly with the observed ones. Nevertheless, it is encouraging to find that such simple model for stellar convection zone is capable of reproducing the basic features of line bisectors and their variation with the spectral type of stars. The variation in bisector shape with the line strength and excitation potential could be due to differences in the amplitudes of velocity and flux fluctuations. The amplitude of velocity fluctuations will

change with the height of formation, while the amplitude of flux fluctuations could be different due to variation in excitation potential of the lines.

Although we have not computed the models for other stars studied by Dravins (1987), on the basis of our results we may speculate that for the hot stars like Canopus and Sirius the line bisector shape could result from modes with moderate or large values of l with same phase relations as for Procyon, but with larger amplitude for the vertical velocity. Further, on the basis of our convection zone models we can speculate that the length

and time scales for granulation and supergranulation for α Cen A are somewhat larger than those for the Sun. For the cool giant Arcturus the length scales for dominant convective cells are very large, being a significant fraction of the stellar radius.

It is a pleasure to thank Professor S. M. Chitre for fruitful discussion. One of us (S. K. P.) would like to thank the Tata Institute of Fundamental Research for financial support and hospitality during the course of this work.

REFERENCES

- Allen, C. W. 1973, *Astrophysical Quantities* (London: Athlone).
 Antia, H. M., Chitre, S. M., and Narasimha, D. 1983, *M.N.R.A.S.*, **204**, 865.
 ———. 1984, *Ap. J.*, **282**, 574.
 Beckers, J. M., and Nelson, G. D. 1978, *Solar Phys.*, **58**, 243.
 Bell, R. A., Edvardsson, B., and Gustafsson, B. 1985, *M.N.R.A.S.*, **212**, 497.
 Bray, R. J., and Loughhead, R. E. 1978, *Pub. A.S.P.*, **90**, 609.
 Dravins, D. 1982, *Ann. Rev. Astr. Ap.*, **20**, 61.
 ———. 1987, *Astr. Ap.*, **172**, 211.
 ———. 1988, in *Solar and Stellar Granulation*, R. J. Rutten and G. Severino (in press).
 Dravins, D., Lindgren, L., and Nordlund, Å. 1981, *Astr. Ap.*, **96**, 345.
 Dravins, D., and Nordlund, Å. 1986, *Bull. AAS*, **18**, 1002.
 Gray, D. F. 1980, *Ap. J.*, **235**, 508.
 ———. 1981, *Ap. J.*, **251**, 583.
 Gray, D. F., and Toner, C. G. 1985, *Pub. A.S.P.*, **97**, 543.
 Mihalas, D. 1978, *Stellar Atmospheres* (San Francisco: Freeman).
 Narasimha, D., and Antia, H. M. 1982, *Ap. J.*, **262**, 358.
 Nordlund, Å. 1982, *Astr. Ap.*, **107**, 1.
 Schröter, E. H. 1957, *Zs. Ap.*, **41**, 141.

H. M. ANTIA: Theoretical Astrophysics Group, Tata Institute of Fundamental Research, Homi Bhabha Road, Bombay 400 005, India

S. K. PANDEY: Department of Physics, Ravishankar University, Raipur 492 010, India